IV.6. PROMOTED IRON FISCHER-TROPSCH CATALYSTS. CHARACTERIZATION BY NITROGEN SORPTION (Diane R. Milburn, Komandur V. R. Chary and Burtron H. Davis).

IV.6.1. ABSTRACT

The effects of promoters on BET surface area and porosity of precipitated iron catalysts are examined. A series of metal oxide promoted iron catalysts was prepared by coprecipitation of the nitrate salts to produce 6% by weight of promoter oxide. Surface areas and pore volumes tend to decrease with increasing promoter ionic radius although there is essentially no change in the shape of the nitrogen isotherm or pore size distribution. Addition of alkali (K) or alkaline-earth (Ca) to silica or alumina promoted iron catalysts also results in a decrease in surface area and pore volume with increasing metal loading. The presence of alkali or alkaline-earth appears to impede crystallization during heating.

IV.6.2. INTRODUCTION

Iron based catalysts are widely used in the ammonia synthesis (IV.6.1) and the Fischer-Tropsch synthesis of hydrocarbons from CO and H_2 (IV.6.2). Alkali promoters are frequently added to these catalysts to improve activity, selectivity and/or life. In addition, structural promoters, such as SiO_2 or Al_2O_3, may be added to the catalyst to improve or maintain surface area and to extend the catalyst lifetime.

Emmett and coworkers (IV.6.3-IV.6.6) conducted a series of chemisorption studies directed toward developing an understanding of the nature of the promoters in these catalysts. These studies led to the conclusion that both types of promoters are present on the catalyst surface. In the low surface area ammonia synthesis catalysts

the alumina or silica promoters appear to be present on the surface of the iron metal, and to form islands that occupy about half of the surface of the metallic iron. Alkali was viewed to be present both on the surface of the iron and of the alumina or silica. This picture of the ammonia synthesis catalyst persists even today. The structure of the Fischer-Tropsch synthesis catalyst is less well known because of the complication caused by the actual, or potential, presence of one or more bulk or surface iron carbides (IV.6.7).

Dry (IV.6.8) reported that the surface area and the pore volume were the major factors in determining the properties of the Fischer-Tropsch synthesis catalyst. Thus, the initial surface area and pore volume are important factors in the preparation of precipitated iron Fischer-Tropsch synthesis catalysts. This study examines the effects on surface area and porosity resulting from the addition of a variety of metal oxide promotors and of increased loadings of alkali (K) or alkaline-earth (Ca) promotors on a precipitated iron catalyst containing 6 wt.% alumina or silica.

IV.6.3. EXPERIMENTAL

Unpromoted $Fe(OH)_3$ was prepared by the precipitation of Fe^{III} nitrate with ammonium hydroxide at pH=8. The resulting dark brown precipitate was then filtered and washed four times with distilled deionized water prior to drying in flowing air at 100°C for 24 hours. Metal oxide promoted samples were prepared under similar conditions using a 15.6M ammonium hydroxide solution to precipitate from a solution of iron nitrate and the appropriate metal nitrate. In several cases the pH exceeded 8.5. The silica promoted iron was coprecipitated from iron nitrate and silica gel, prepared from the hydrolysis of tetraethylorthosilane. Promoter loadings were 6% by

weight based on the stable oxide following calcination in air. Some physical properties of these samples are summarized in Table IV.6.1. Potassium and calcium were added to the 6% Al_2O_3 and 6% SiO_2 promoted samples by incipient wetness using solutions of potassium nitrate or calcium nitrate. Alkali loadings were 2%, 4% and 6% by weight. Another set of doubly promoted samples were prepared by sequential incipient wetness corresponding to 2% K , 2% Ca; 4% K, 4% Ca and 6% K, 6% Ca on the 6% Al and the 6% Si promoted iron oxides. All samples were dried in flowing air at 100°C for 12 hours and portions of each alkali or alkaline-earth promoted sample were calcined in air at 300°C for 6 hours in order to examine the effects of temperature.

X-ray powder diffraction patterns were obtained using a Phillips model 3100 instrument with a CuKα radiation source. The instrument is designed to effect automatic sample changes and the equipment introduces a peak at 2θ = 44.6 for iron. Thus, this peak should be ignored in the XRD patterns.

Nitrogen sorption isotherms were measured using a Quantachrome Autosorb 6 instrument. Prior to analysis, each sample was outgassed at 80°C at <50 mtorr for at least 12 hours. BET surface areas were calculated from the adsorption branch of the isotherms and pore size distributions were calculated from the desorption branch using the model of Broekhoff and deBoer assuming cylindrical pores (IV.6.9).

IV.6.4. RESULTS

A series of catalysts were prepared to contain 6 wt.% of the metal oxide used as the non-reducible promoter. The BET surface areas of these singly promoted iron oxide catalysts show a uniform trend with the ionic radius of the promoter metal

(Figure IV.6.1). In this paper we refer to the material as an iron oxide although the materials, even after calcination at 300°C, are amorphous to X-ray examination. As shown in Figure IV.6.1, promoters with a considerably smaller ionic radius that Fe^{3+} produce a material with a surface area that is greater (by nearly 50%) than that of the unpromoted iron oxide. As the ionic radius of the metal ion of the promoter approaches that of Fe^{3+} the surface area undergoes a rapid decrease to that of the unpromoted iron oxide. As the ionic radius of the metal ion of the promoter becomes greater than that of Fe^{3+} the surface area of the promoted iron oxide shows a sharp decrease. For promoters with an ionic radius of about 0.75Å and larger the surface area approaches a constant value that is about 75% of that of the unpromoted iron oxide. Thus, there is a clear relationship between the surface area of the promoted iron oxide catalyst precursor and the ionic size of the metal of the promoter.

Since the catalyst precursors have been prepared to contain a constant wt.% of metal oxide promoter, there is a considerable variation in the moles of promoter metal per gram of catalyst. However, as shown in Figure IV.6.2, there is only a slight increase in the BET surface area with increasing moles of promoter metal.

The presence of the metal oxide promoter does not make a significant change in either the type of adsorption/desorption isotherms or the hysteresis loop; this is true for both the group of promoters that lead to a larger (Figure IV.6.3) or smaller (Figure IV.6.4) surface area than the unpromoted iron oxide. A Type IV adsorption isotherm is obtained in all cases and the hysteresis loop is Type H2 for all of the samples (IUPAC classification (IV.6.10)). Each isotherm exhibits a clear limiting adsorption showing a filling of the pore structure; this permits an estimation of the pore volume

from the "so-called" Gurvitsch Rule (IV.6.11). The total pore volumes calculated using the model of Broekhoff and deBoer assuming cylindrical pores appears to show a slight decrease with increasing ionic radius of the metal promoter; however, there is considerable scatter for the data if there is such a trend (Figure IV.6.5). The pore volume estimated using the Gurvitsch Rule exhibits the same trend as obtained with the Broekhoff-deBoer model (Figure IV.6.6); however, the Broekhoff-deBoer model returns a total pore volume that is about 1.5 times as great as those from the Gurvitsch Rule.

The pore volume of the materials is contained primarily in pores in the range of 20-27Å except for the ones promoted by Th and Zr; these two catalyst precursors appear to have a slightly larger radius for the maximum pore size (Figure IV.6.7).

The incorporation of silica into the catalyst precursor causes an increase in the surface area (Figure IV.6.8) as the ratio Si/(Si + Fe) increases up to about 6 atomic %. The incorporation of silica beyond about 6 atomic % does not cause a further increase in the surface area. A similar trend is observed for the alumina promoted catalyst precursor except that the lower loading of the promoter appears to have a greater impact upon increasing the surface area (Figure IV.6.9).

Potassium or calcium was added to portions of an alumina or silica promoted iron oxide sample to produce materials that contain 2, 4, or 6 atomic % of the alkali or alkaline-earth promoter. Following impregnation, the samples were dried at 100°C. The addition of K^+ or Ca^{2+} to the iron oxide caused the surface area to decrease, and the decrease became greater as the amount of promoter increased (Figure IV.6.10). Except for the lowest loading, Ca^{2+} caused a greater decrease of the surface area

than K^+ did. Another series of catalyst precursors were prepared by first impregnating with K^+ to 2, 4 or 6 atomic %, dried at 100°C, and then impregnated with 2, 4 or 6 atomic % Ca^{2+}. The surface area of the material containing both promoters had a lower surface area than a material containing the same atomic % of the single promoter. Surprisingly, the surface area of the K^+ or Ca^{2+} promoted materials does not depend upon the level of the alkali or alkaline-earth promoter. However, the surface area of the material promoted with both the alkali and alkaline-earth promoter does decrease with the loading of the promoter. The results obtained for the promoted silica promoted iron oxide (Si/(Si + Fe) = 0.6) were very similar to those shown in Figure IV.6.10 for the alumina promoted materials. The addition of Ca^{2+} (Figure IV.6.11) does not alter the type of isotherm or the hysteresis loop; similar results were obtained for the materials promoted with K^+. Likewise, the pore size distribution did not vary with the level of K^+ or Ca^{2+}, even when the iron oxide contained equal amounts of K^+ and Ca^{2+}. The surface areas of the doubly promoted catalysts are summarized in Table IV.6.2.

The iron oxide following precipitation and drying at 100°C was amorphous to X-rays. However, the unpromoted material following calcination at 300°C was α-Fe_2O_3 (Figure IV.6.12). The incorporation of even 1 atomic% Si to the precipitated material retards the crystallization to a material that gives an X-ray diffraction pattern for a crystalline material. The impregnation of the precipitate with 0.06 atomic fraction silicon with potassium up to 6 atomic % did not lead to a crystalline material following calcination at 300°C for 4 hours. All of the Al promoted iron oxides were amorphous following drying at 100°C. However, Al was less effective for preventing the

crystallization following heating at 300°C for 4 hours; samples containing less that 0.03 atomic fraction Al are crystalline following calcination (Figure IV.6.13). The addition of K^+ to the aluminium promoted iron oxide (Al/(Al + Fe) = 0.06) even to 6 atomic % did not lead to a crystalline material following calcination at 300°C.

IV.6.5. DISCUSSION

While it is apparent that the addition of a promoter will alter the surface area of precipitated iron oxide and that this effect depends upon the ionic radius of the promoter, it is not readily apparent why this should be the case. It is well established that the incorporation of an anion on the surface of zirconia will aid in retaining the surface area and inhibiting the crystallization. For example, the presence of the sulfate anion may increase the crystallization temperature by 100°C or even more; the surface area of the calcined material may be as much as 150% greater than the material that does not contain sulfate (IV.6.12). In the case of the sulfated zirconia, it has been demonstrated that the sulfate retards the tetragonal to monoclinic phase transformation by inhibiting the adsorption of oxygen (IV.6.13).

In the preparation of the iron oxide catalyst precursors, the promoter was incorporated by co-precipitation. At least some of the metal promoters can be incorporated into the structure of the crystalline iron oxide that is produced following calcination. However, the precipitated material is amorphous to X-rays even following drying at 100°C. It therefore appears likely that the promoter operates in a manner that is similar to that of sulfate in the case of zirconia. Many, or even all, of the promoters listed in Table IV.6.1 will be present as the oxygen containing anion, such as CrO_3^-, at the pH where precipitation was effected. Thus, it appears that adsorption

of the anion on the surface of the amorphous, hydrated iron oxide is likely. It therefore appears that the presence of the promoter, adsorbed as the anion, is responsible for the inhibition of the crystallization and the impact upon the surface area. If this view is correct, then it is necessary for the anion of the promoters with a small ionic radius to be adsorbed very strongly and to exhibit a maximum effect, presumably by maximizing the surface coverage. The promoters with the large ionic radius, due either to a lower tendency to form the anion or, more likely, to the formation of three dimensional precipitates, lead to a lower surface coverage.

IV.6.6. ACKNOWLEDGMENT

The authors acknowledge the financial support of this work by the Department of Energy contract No. DE-AC22-91PC90056 and by the Commonwealth of Kentucky.

IV.6.7. REFERENCES

IV.6.1. P. H. Emmett in "The Physical Basis of Heterogeneous Catalysis," (E. Drauglis and R. I. Jaffee, eds.), Plenum Press, New York, 1975, pg. 3.

IV.6.2. F. Fischer and H. Tropsch., *Ges. Abhandl. Kenntnis Kohle*, **10**, 335 (1930).

IV.6.3. P. H. Emmett and S. Brunauer, *J. Am. Chem. Soc.*, **56**, 35 (1934).

IV.6.4. P. H. Emmett and R. W. Harkness, *J. Am. Chem. Soc.*, **57**, 1624 (1935).

IV.6.5. P. H. Emmett and S. Brunauer, *J. Am. Chem. Soc.*, **59**, 310 (1937).

IV.6.6. S. Brunauer and P. H. Emmett, *J. Am. Chem. Soc.*, **62**, 1732 (1940).

IV.6.7. G. B. Raupp and W. N. Delgass, *J. Catal.*, **58**, 361 (1979).

IV.6.8. M. E. Dry, in "Catalysis," (J. R. Anderson and M. Boudart, eds.), Springer-Verlag, Berlin, 1981, pg. 182.

IV.6.9. J. C. P. Broekhoff and J. H. deBoer, *J. Catal.*, **10**, 368 (1968).

IV.6.10. K. S. W. Sing, D. H. Everett, R. A. W. Haul, L. Moscou, R. A. Pierotti, J. Rouquerol and T. Siemineiewska, *Pure & Appl. Chem.*, **57**, 603 (1985).

IV.6.11. L. Sliwinska and B. H. Davis, *Ambix*, **34**, 81 (1987).

IV.6.12. S. Chokkaram, R. Srinivasan, D. Milburn and B. H. Davis, *J. Colloid Surf. Sci.*, **165**, 160 (1994).

IV.6.13. R. Srinivasan, T. Watkins, C. Hubbard and B. H. Davis, submitted.

Table IV.6.1

Effects of Metal Promoter Addition on Surface Area and Pore Volume of Precipitated Iron Catalyst Precursors

Promoter	Precursor	Ion	Ionic Radius (Å)	Surface Area (m^2g^{-1})	Pore Volume (cm^3g^{-1})
B_2O_3	Boric Acid	B^{3+}	0.20	315	0.244
SiO_2	Tetraethyl orthosilane	Si^{4+}	0.41	329	0.291
Al_2O_3	Aluminum^{III} nitrate	Al^{3+}	0.50	274	0.233
MnO_2	Manganese^{III} nitrate	Mn^{2+}	0.54	262	0.254
V_2O_5	Ammonium metavanadate	V^{5+}	0.59	231	0.214
MoO_3	Ammonium heptamolybdate	Mo^{6+}	0.62	221	0.210
None	-----	Fe^{3+}	0.64	240	0.260
MgO	Magnesium nitrate	Mg^{2+}	0.65	210	0.189
WO_3	Ammonium metatungstate	W^{6+}	0.68	223	0.212
Cr_2O_3	Chromium^{III} nitrate	Cr^{3+}	0.69	215	0.207
ZrO_2	Zirconium oxynitrate	Zr^{4+}	0.79	171	0.247
CaO	Calcium nitrate	Ca^{2+}	0.99	164	0.162
ThO_2	Thorium nitrate	Th^{2+}	0.99	176	0.223
BaO	Barium nitrate	Ba^{2+}	1.35	165	0.179

Table IV.6.2

Impact of K^+ and/or Ca^{2+} Promoters on Surface Area and Pore Volume of Dried (100°C) or Calcined (300°C) Silicon or Aluminum Containing Precipitated Iron Catalyst Precursors

		Dried, 100°C		Calcined 300°C	
Silicon Atomic %	Promoter (atomic %)	Surface Area m^2/g	Pore Volume m^2/g	Surface Area m^2/g	Pore Volume m^2/g
1	Ca (0)	251	0.24		
1	Ca (0.33)	240	0.23		
1	Ca (0.66)	255	0.24		
1	Ca (1)	229	0.21		
3	Ca (0)	264	0.23		
3	Ca (1)	248	0.23		
3	Ca (2)	214	0.20		
3	Ca (3)	272	0.21		
6	Ca (0)	329	0.25		
6	Ca (2)	264	0.21	251	0.24
6	Ca (4)	262	0.20	220	0.20
6	Ca (6)	178	0.14	221	0.21
6	Ca (2) K (2)	257	0.23	201	0.22
6	Ca (4) K (4)	180	0.19	173	.19

		Dried, 100°C		Calcined 300°C	
Silicon Atomic %	Promoter (atomic %)	Surface Area m^2/g	Pore Volume m^2/g	Surface Area m^2/g	Pore Volume m^2/g
6	Ca (6) K (6)	147	0.14	129	0.14
6	K (2)	306	0.26	231	0.24
6	K (4)	234	0.20	202	0.21
6	K (6)	241	0.19	203	0.21
Aluminum Atomic %					
6	K (2)	247	0.20	166	0.20
6	K (4)	240	0.22	175	0.19
6	K (6)	186	0.15	150	0.17
6	Ca (2)	260	0.23	180	0.21
6	Ca (4)	247	0.20	156	0.19
6	Ca (6)	145	0.11	160	0.17
6	Ca (2) K (2)	225	0.20	101	0.12
6	Ca (4) K (4)	178	0.15	144	0.16
6	Ca (6) K (6)	113	0.11		

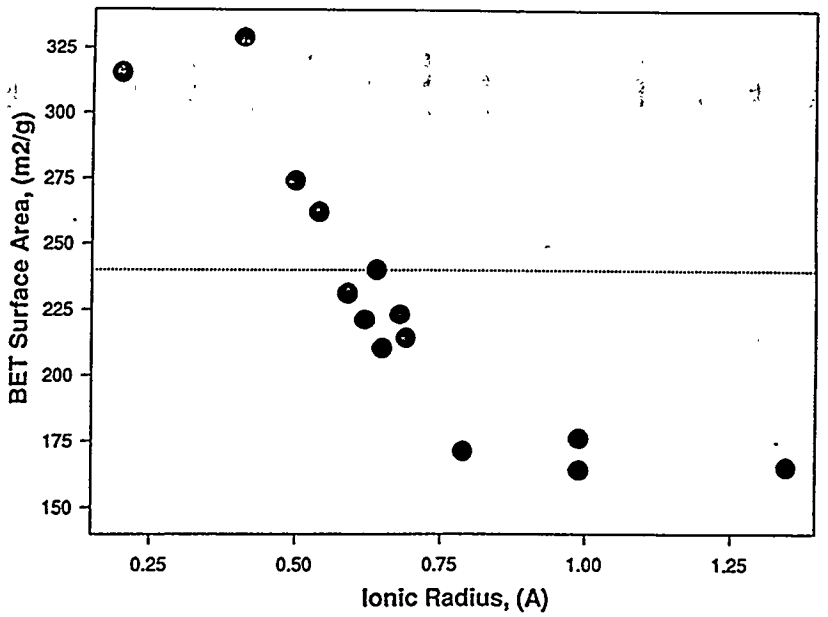

Figure IV.6.1. The dependence of the surface area of the catalyst precursor upon the ionic size of the metal promoter (dotted line indicates the value of the unpromoted iron oxide).

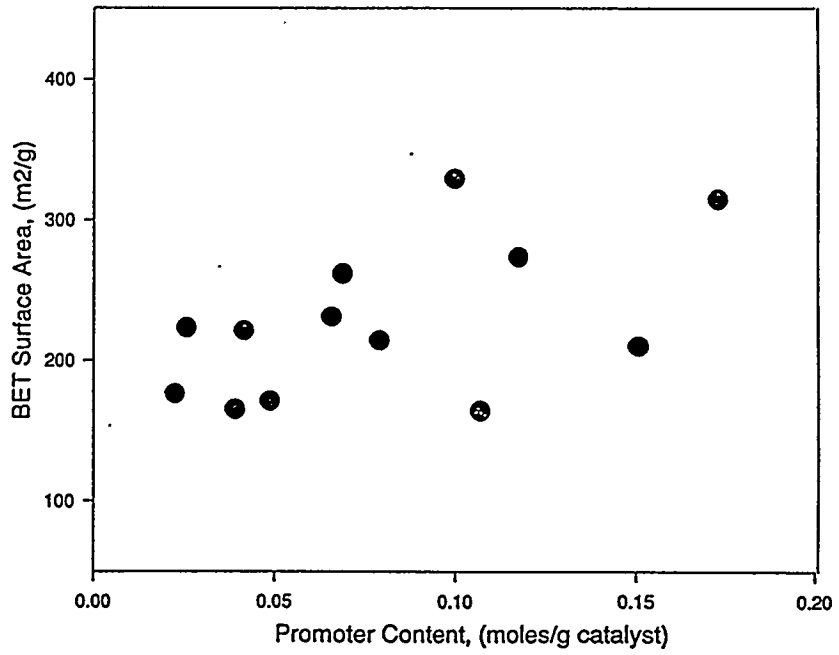

Figure IV.6.2. The dependence of the surface area of the catalyst precursor on the moles of promoter per gram of material.

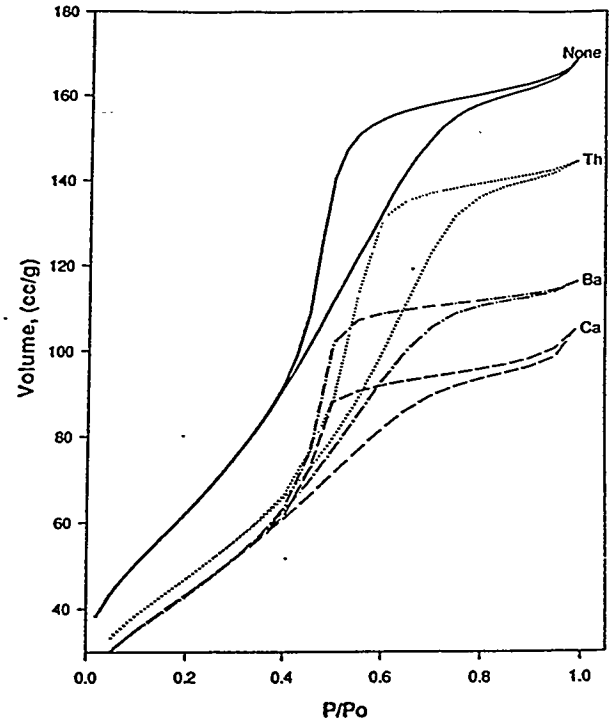

Figure IV.6.3. Adsorption/desorption isotherms for iron oxide and materials promoted by metal oxides with an metal ionic radius larger than Fe^{3+}.

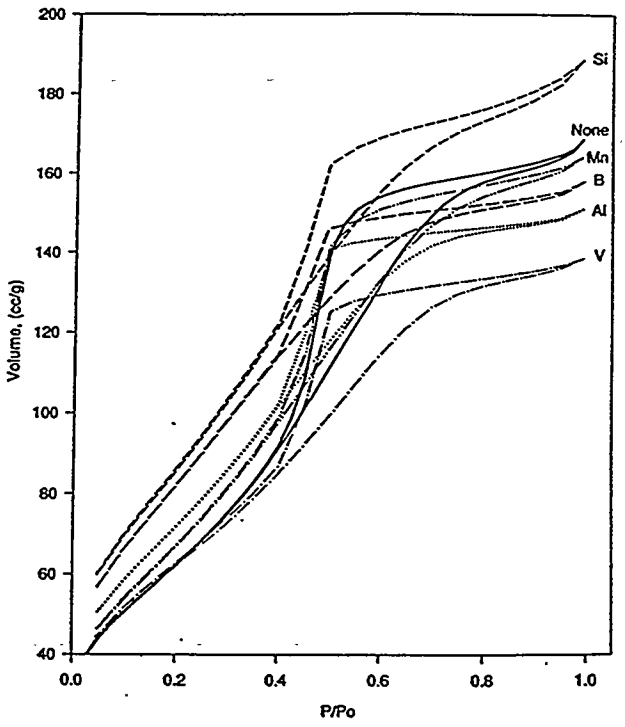

Figure IV.6.4. Adsorption/desorption isotherms for iron oxide and materials promoted by metal oxides with a metal ionic radius smaller than Fe^{3+}.

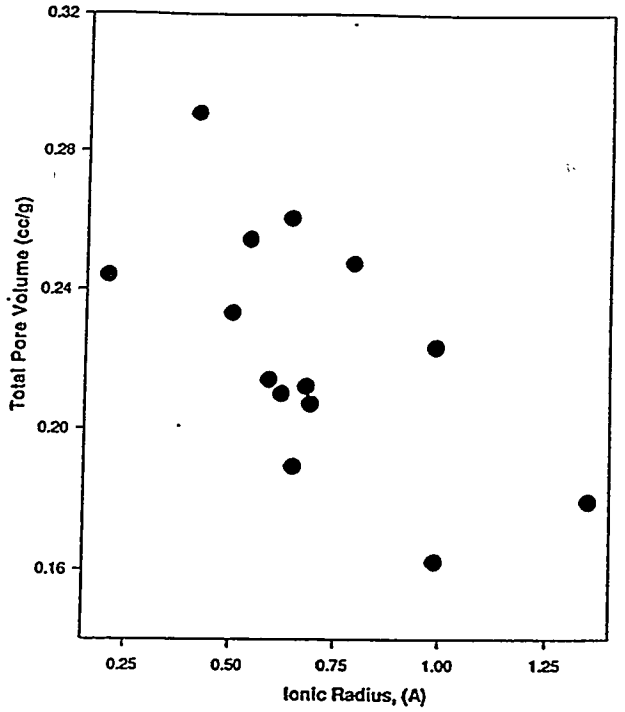

Figure IV.6.5. The dependence of the total pore volume (Broekhoff-deBoer cylindrical pore model) of promoted iron oxide catalyst precursors on the ionic radius of the promoter metal.

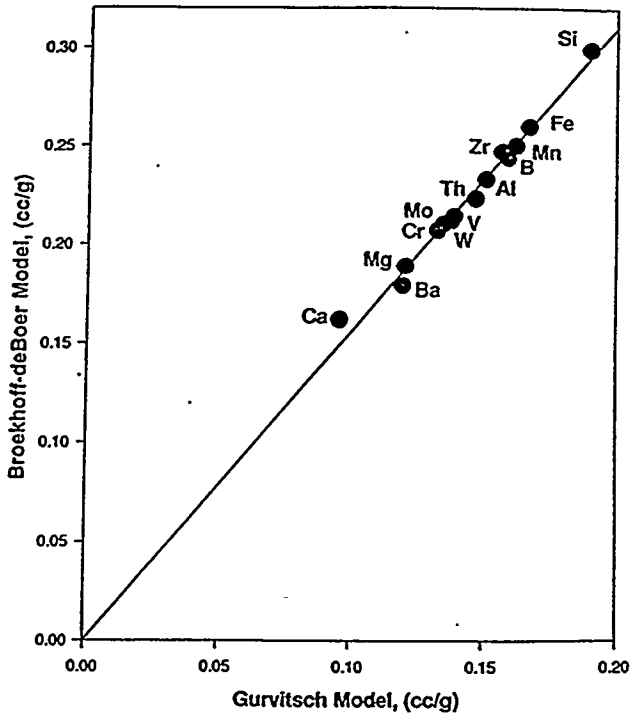

Figure IV.6.6. Comparison of the total pore volume calculated using the Broekhoff-deBoer cylindrical pore model and the Gurvitsch pore volume.

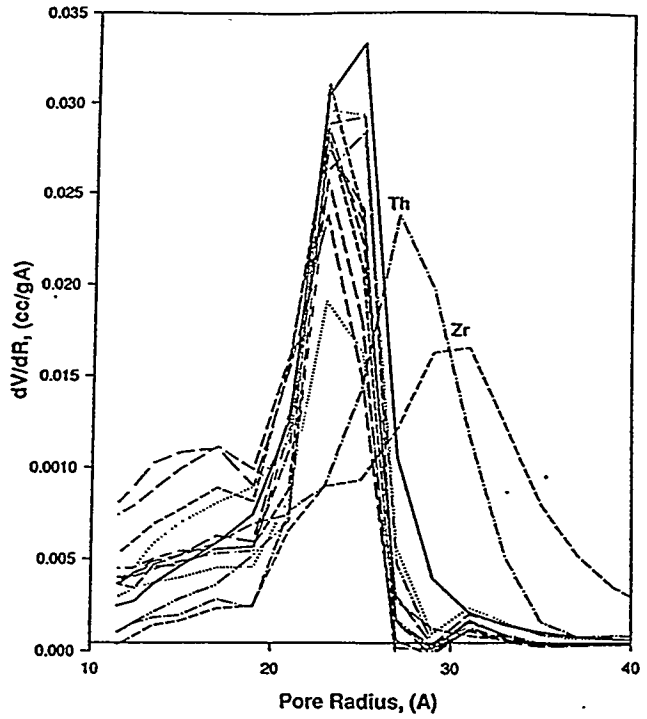

Figure IV.6.7. The pore size distributions for promoted iron oxides.

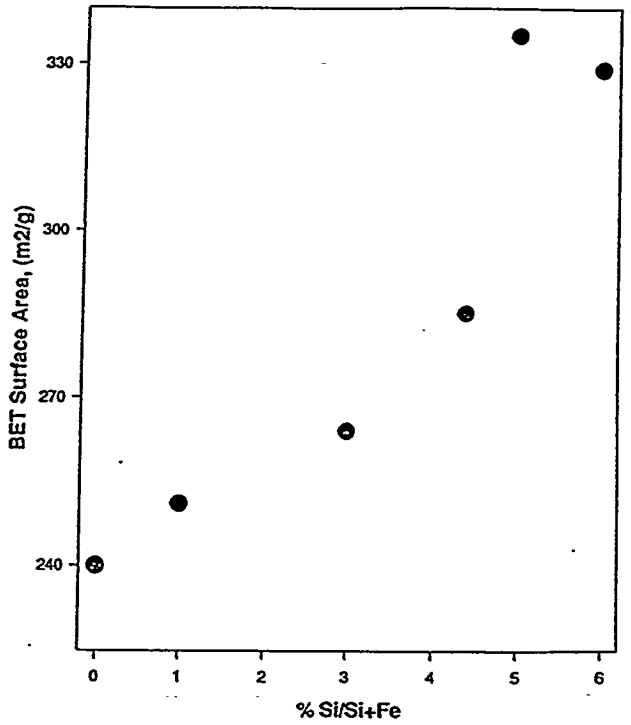

Figure IV.6.8. Variation of the surface area of the catalyst precursor with increasing silica content.

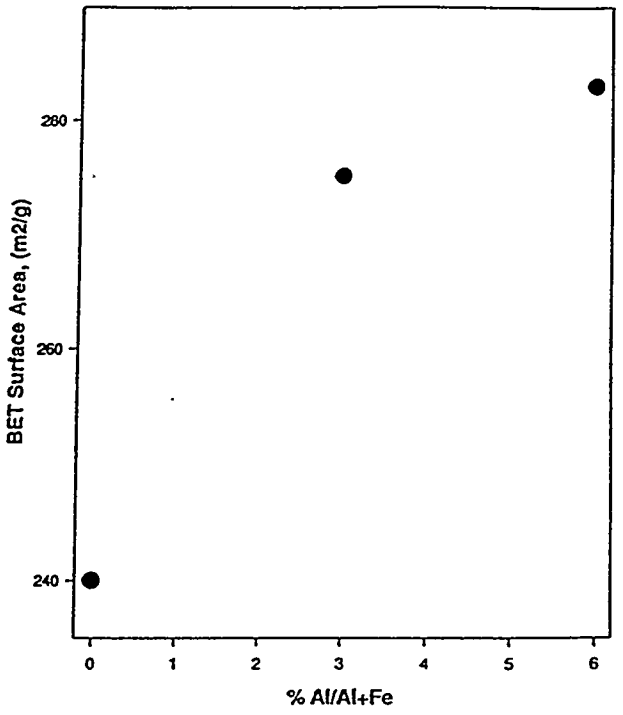

Figure IV.6.9. Variation of the surface area of the catalyst precursor with increasing alumina content.

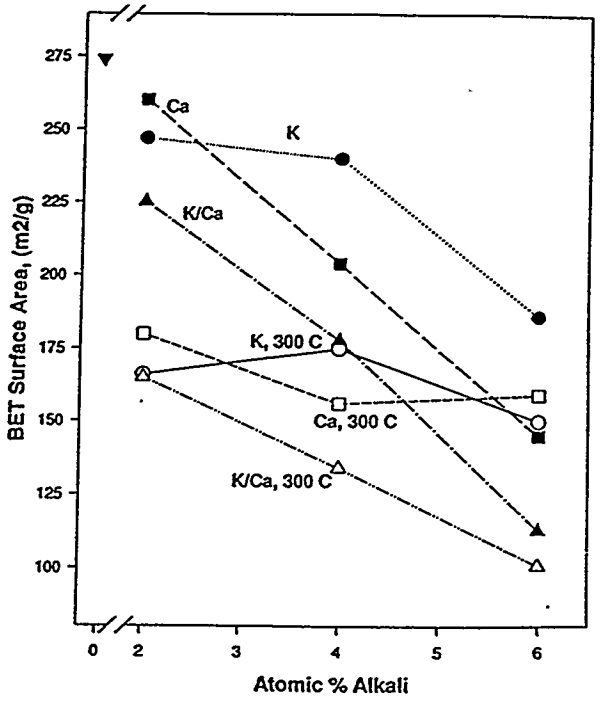

Figure IV.6.10. BET surface area of an alumina promoted iron oxide (Al/(Al + Fe) = 0.06) with increasing amounts of K^+, Ca^{2+} or (K^+ + Ca^{2+}) following drying at 100°C or calcination at 300°C.

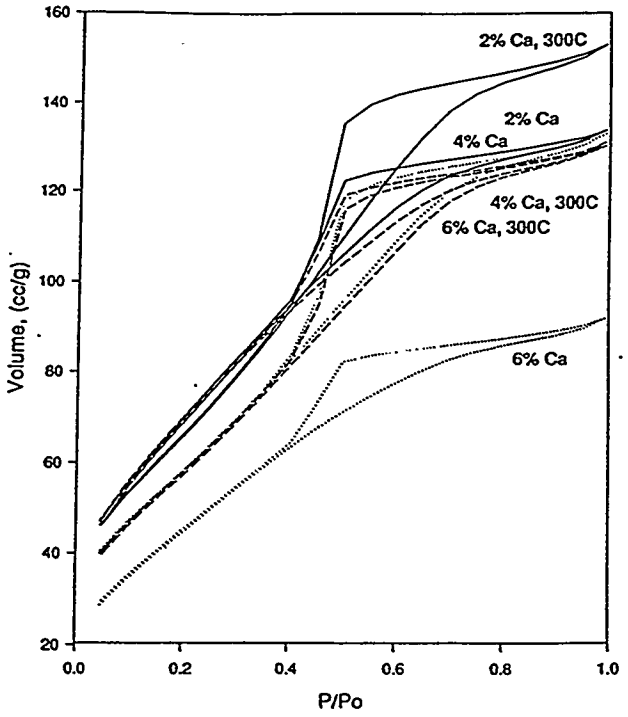

Figure IV.6.11. Nitrogen adsorption/desorption isotherms for silica promoted iron oxides with increasing amounts of Ca^{2+} following drying at 100°C and calcination at 300°C.

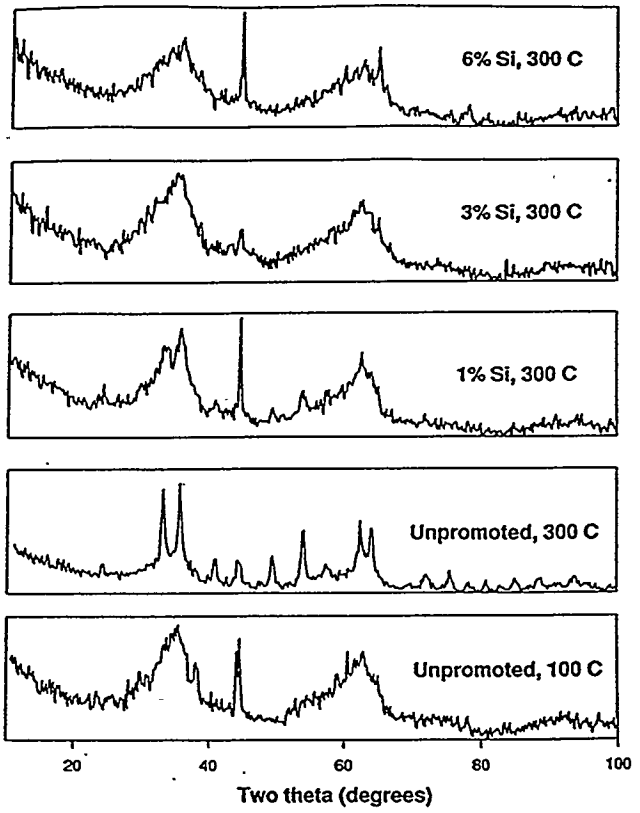

Figure IV.6.12. X-ray diffraction patterns for unpromoted and silica promoted iron oxides.

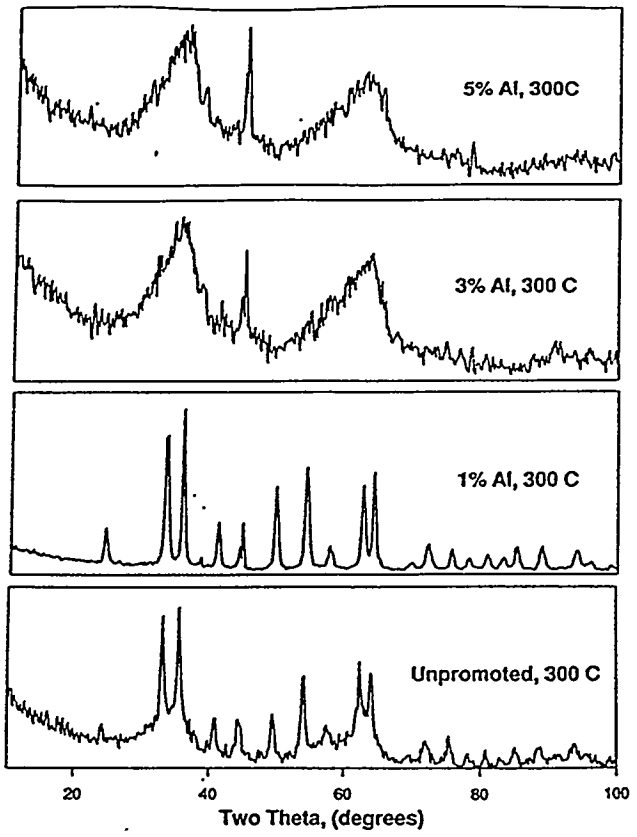

Figure IV.6.13. X-ray diffraction patterns for unpromoted and alumina promoted iron oxide following calcination at 300°C.